

Influence of carrier lifetime on quantum criticality and superconducting T_c of $(\text{TMTSF})_2\text{ClO}_4$

Abdelouahab Sedeki,¹ Pascale Auban-Senzier,² Shingo Yonezawa,³ Claude Bourbonnais,⁴ and Denis Jerome²

¹*Université Dr Tahar Moulay Saida, BP 138 cité ENNASR 20000, Saida, Algeria.*

²*Laboratoire de Physique des Solides (UMR 8502), Univ.Paris-Sud, 91405 Orsay, France*

³*Department of Physics, Graduate School of Science, Kyoto University, Kyoto 606-8502, Japan*

⁴*Regroupement Québécois sur les Matériaux de Pointe and Institut Quantique, Département de physique, Université de Sherbrooke, Sherbrooke, Québec, Canada, J1K-2R1*

(Dated: March 26, 2022)

This work presents and analyzes electrical resistivity data on the organic superconductor $(\text{TMTSF})_2\text{ClO}_4$ and their anion substituted alloys $(\text{TMTSF})_2(\text{ClO}_4)_{1-x}(\text{ReO}_4)_x$ along the least conducting c^* axis. Nonmagnetic disorder introduced by finite size domains of anion ordering on non Fermi liquid character of resistivity is investigated near the conditions of quantum criticality. The evolution of the T -linear resistivity term with anion disorder shows a limited decrease in contrast with the complete suppression of the critical temperature T_c as expected for unconventional superconductivity beyond a threshold value of x . The resulting breakdown of scaling between both quantities is compared to the theoretical predictions of a linearized Boltzmann equation combined to the scaling theory of umklapp scattering in the presence of disorder induced pair-breaking for the carriers.

I. INTRODUCTION

Quantum criticality that becomes unstable against the emergence of superconductivity is a common feature of most recent unconventional superconductors. It happens when the ordering temperature of an antiferromagnetic phase (AFM), which can be metal-like, semi-metallic or insulating ends towards zero temperature, as a control parameter doping or pressure is varied¹. Such is the situation encountered in the vast family of pnictide superconductors^{2,3}. That may also be the situation met in hole doped cuprates although there, the quantum critical point (QCP) corresponding to the termination at zero temperature of the pseudogap phase is beneath the superconducting dome of their phase diagram⁴. This is also found in electron doped cuprates and heavy fermions superconductors, which both exhibit an AFM phase terminating toward zero temperature when the electron doping level or pressure are varied respectively in the former⁵ or latter compounds^{6,7}. The proximity of an AFM Mott insulating phase to superconductivity is also present in layered organic superconductors bearing much resemblance with the phase diagram of cuprates⁸⁻¹⁰.

Most experimental investigations performed near QCP conditions have revealed that several physical properties deviate significantly from the canonical Fermi liquid behaviour, in particular the resistivity which instead of the expected T^2 dependence exhibits a linear- T dependence¹¹, a puzzling feature shared by essentially all the aforementioned unconventional superconductors close to a magnetic QCP.

Moreover, there exists another class of materials displaying both antiferromagnetism and superconductivity that has not been as much highlighted namely, the quasi-one dimensional (Q1D) Bechgaard organic superconductors^{12,13}. Although superconductivity in heavy fermions¹⁴ has been discovered before that in Q1D

organics, it is in these latter materials that superconductivity first revealed following the suppression of an insulating phase under pressure which was subsequently identified as a spin density wave (SDW) state¹⁵⁻¹⁷. A strong argument in favour of Q1D superconductors is the relative simplicity of their electronic structure, comprising a single nearly flat Fermi surface as well as a temperature-pressure phase diagram which can be considered as a textbook example of magnetic quantum criticality that becomes unstable to the formation of superconductivity^{18,19}.

An unusual behavior of metallic transport in $(\text{TMTSF})_2\text{PF}_6$ under pressure at low temperature has been observed in the first studies¹⁵ related to a pronounced T -linear tendency between 0.1 K and 10 K and even a downward curvature of the resistivity in the pressure range corresponding to the vicinity of the QCP²⁰. While superconducting fluctuations were first considered as a possible interpretation in the 3D temperature regime very close to T_c where the transverse coherence length is larger than the interstack distance, paraconductivity from superconducting origin failed to account for the correct temperature dependence observed up to 10K or so²⁰. Thirty years have been required to clarify the problem when similar behaviors of transport have been detected in other superconductors close to a QCP in particular in cuprates and pnictides^{4,11}.

As far as organic superconductors are concerned, detailed investigations of transport at low temperature has been conducted first on $(\text{TMTSF})_2\text{PF}_6$ under pressure²¹. In this case the temperature dependence of the inelastic scattering in conditions very close to the QCP is a clear cut behavior. $\rho(T)$ follows a T -linear law over a decade in temperatures above T_c , already visible on log-log plot of the resistivity. The behavior is becoming quadratic as expected in a Fermi liquid above 10 K²¹. However, as the location of the compound in the $T - P$

arXiv:1806.06395v1 [cond-mat.str-el] 17 Jun 2018

phase diagram is moved away from the QCP conditions the resistivity acquires a quadratic component even at low temperature and becomes fully quadratic when T_c is suppressed. The log-log plot of the resistivity reveals a power law $\Delta\rho \propto T^\beta$ with an exponent β evolving from 1 to 2 between 11.8 and 20.8 kbar²¹. Subsequently, an other procedure has been followed to analyse the inelastic scattering of $(\text{TMTSF})_2\text{PF}_6$ namely, a sliding fitting procedure²² with a second order polynomial form such as $\rho(T) = \rho_0 + A(T)T + B(T)T^2$. Here, the fitting procedure enables the detection of a possible temperature dependence of the A and B prefactors, whereas the value of ρ_0 depends on pressure only²². This procedure has shown that the T -linear contribution is dominant below 10 K compared to the Fermi liquid contribution close to the QCP, but otherwise becomes of the order of the quadratic contribution.

The same log-log analysis failed to provide a clear cut picture in $(\text{TMTSF})_2\text{ClO}_4$, but the polynomial fitting procedure conducted on the resistivity along c^* , led to conclusions that A and B are only weakly temperature dependent in this compound between T_c and 15 K (though still pressure dependent)²³. The detailed analysis of the temperature dependent resistivity over an extended range of pressures has shown that $\rho_{c^*}(T)$ can thus be fitted to the polynomial expression $\rho_{c^*0} + AT + BT^2$ where all parameters are evolving under pressure but the experimental feature, $A \rightarrow 0$ as $T_c \rightarrow 0$ is preserved²³.

Although a precise functional relation between A and T_c is uncertain, the salient result of these pressure studies is the existence of a T -linear contribution to the resistivity being finite only when T_c is finite, suggesting in turn the existence of a common origin for pairing and the T -linear inelastic scattering²².

While there is no general consensus about the microscopic origin of T -linear resistivity appearing near a QCP²⁴, theoretical efforts have been displayed to shed some light on its origin in the context of the Q1D Bechgaard salts^{19,25,26}. The electron-electron scattering rate, as extracted from the imaginary part of the one-particle self-energy, has been derived by a renormalisation group procedure. The calculation that takes into account the quantum interference between electron-electron and electron-hole scattering channels was able to link the strength of the linear resistivity term to the one of pairing as a function of pressure¹⁹. Another strategy has been to connect the solution of the transport Boltzmann equation to the renormalization group approach to non conserving momentum scattering amplitudes. This procedure has confirmed the existence of a T -linear term in resistivity and the correlation between its strength and the size of superconductivity pairing.²⁶

These findings have motivated the present work devoted both experimentally and theoretically to the influence of a finite elastic life time on the T -linear resistivity in the Bechgaard salts. On the theoretical side impurity scattering, assumed to be absent so far in the renormalization group calculations of the scattering amplitudes,

is a source of pair breaking for both unconventional superconductivity and density-wave correlations. We will show that this affects to a certain extent the constructive interference between both types of correlations at low energy. Although this can be sufficient for the complete suppression of T_c , it turns out that SDW correlations that build up at higher energy are less affected by disorder induced pair-breaking and remain relatively strong in amplitude. As the source of umklapp scattering for carriers in the Boltzmann equation, these correlations sustain to a great extent the non Fermi liquid character of resistivity in spite of the scaling breakdown between the T -linear term and T_c .

On experimental side, previous investigations have shown that T_c in the $(\text{TMTSF})_2X$ series is strongly affected by disorder of non magnetic origin²⁷⁻³⁰, providing in turn some hint for the existence of a non conventional superconducting gap displaying both signs over the Fermi surface in this spin singlet superconductor³¹, pointing for instance to d -wave (or g -wave) type of superconductivity. As the linear term of transport at low temperature was found to be related to T_c , we feel it is legitimate to test the robustness of the established connection between A and T_c when T_c can be modified by other means but pressure, namely by the influence of non magnetic disorder³². It is worth mentioning that in Sr_2RuO_4 , an equal sensitivity to non magnetic disorder has been observed³³ suggesting that spin triplet pairing is a possible candidate for the SC ground state in this material³⁴.

Fortunately, $(\text{TMTSF})_2\text{ClO}_4$ is the unique system among other superconductors in the $(\text{TMTSF})_2X$ series in which structural disorder can control the elastic scattering time. This property is based on the peculiarity of the tetrahedral symmetry of the anion ClO_4^- .

The structure of $(\text{TM})_2X$ salts belongs to the triclinic space group $P\bar{1}$ with every anion site located on an inversion center. Hence, as long as the local symmetry of anions like PF_6^- is centrosymmetric, their actual orientation always fits the overwhole crystal symmetry. Thus, no additional disorder is introduced. However, non centrosymmetric anions such as tetrahedral ClO_4^- or ReO_4^- may have their oxygen atoms pointing towards methyl groups or Se atoms of one or the other neighboring donor molecules^{35,36}. These (at least two) possible directions lead in turn to a potential source of disorder. While there is no disorder on average at elevated temperature since these tetrahedral anions are rotating as shown by NMR data³⁷, the minimization of entropy due to the reduction of degrees of freedom in thermodynamical equilibrium triggers an anion ordering at low temperature with the concomitant occurrence of a superstructure. In addition, the relative orientation at low temperature of neighboring anions depends on the nature of the anions. For $(\text{TMTSF})_2\text{ReO}_4$, the orientation of ReO_4^- alternates along the three directions providing a periodic lattice distortion of wave vector $(1/2, 1/2, 1/2)$ (in units of reciprocal lattice vector in each direction) with a concomitant metal insulator transition below $T_{\text{AO}} = 176 \text{ K}$ ³⁸, whereas

the alternation of ClO_4^- occurs solely along the b axis in $(\text{TMTSF})_2\text{ClO}_4$ below $T_{\text{AO}} = 24$ K, leading in turn to the $(0,1/2,0)$ order^{39,40}. Such a doubling of periodicity along b is thus responsible for the doubling of the Fermi surface folded along b^* in slowly cooled samples. These samples retain in turn metallic properties at low temperature.

A possible means of introducing controllable disorder in an otherwise well ordered $(\text{TMTSF})_2\text{ClO}_4$ crystal is the substitution of ClO_4^- by ReO_4^- anions. The consequences of the isostructural anion alloying on the electronic properties such as superconductivity have been revealed long ago²⁸, even though the actual structural reasons were not elucidated. For instance, ReO_4^- replacing ClO_4^- in $(\text{TMTSF})_2\text{ClO}_4$ affects T_c so severely that a 1% ReO_4^- concentration is large enough to shift T_c from 1.3 K to 0.9 K and 10% suppresses T_c totally²⁸. Additional investigations of structural and electronic properties of $(\text{TMTSF})_2(\text{ClO}_4)_{(1-x)}(\text{ReO}_4)_x$ have been conducted subsequently^{29,41}. What structural studies have revealed in the ClO_4^- alloys at low concentration of ReO_4^- is the existence of domains in which the $(0,1/2,0)$ ClO_4^- order persists, the size of them controlling the carrier elastic mean free path⁴².

Another way to create defects in $(\text{TMTSF})_2\text{ClO}_4$ is to beat the slow anion orientation process by rapid cooling of the sample, as first detected by NMR, specific heat, EPR and transport measurements⁴³⁻⁴⁵. A recent reinvestigation of magnetic and transport properties of $(\text{TMTSF})_2\text{ClO}_4$ under a well controlled cooling procedure in the vicinity of the anion ordering temperature has revealed at increasing cooling speed above 1 K/mn a cross over from a rather homogenous localized disorder to a granular situation in which anion-ordered puddles are embedded in an anion-disordered background⁴⁶. This picture is reminiscent of the present situation in alloys where the carrier mean free path of the well ordered grains is also limited by their own size.

The fact that the elastic mean free path of $(\text{TMTSF})_2\text{ClO}_4$ can be controlled by disorder is a remarkable property of the material and makes $(\text{TMTSF})_2\text{ClO}_4$ a unique system where to check simultaneously the effect of a change of the mean free path on T_c and on quantum criticality behavior possibly related to the onset of superconductivity²¹.

The present report attends to fulfill this goal with a quantitative study of both superconducting and metallic state properties in two situations where disorder can be introduced with a concomitant control of the mean free path. First, *via* studying lightly ReO_4^- substituted $(\text{TMTSF})_2\text{ClO}_4$ samples and second the fast cooling of pure $(\text{TMTSF})_2\text{ClO}_4$. Theoretically, we broaden the RG approach of the quasi-1D electron gas model to include impurity pair breaking effects on the renormalization of umklapp scattering that enters the linearized Boltzmann equation of electrical transport.

Our study will show that the correlation between the non-Fermi liquid resistivity and T_c , which is well estab-

lished under pressure²¹, breaks down when T_c in this d-wave superconductor is suppressed by non-magnetic disorder. This result emphasizes the strong-pair breaking role of a limited elastic mean free path on T_c as opposed to the much weaker influence on antiferromagnetic fluctuations, which are believed to be a major ingredient for pairing in this superconductor.

In Sec. II, the low temperature transverse resistivity measurements of $(\text{TMTSF})_2(\text{ClO}_4)_{(1-x)}(\text{ReO}_4)_x$ alloys are presented and their superconducting and non-Fermi liquid properties described. Sec. III is devoted to the results of the numerical solution of the linearized Boltzmann equation of resistivity for the Q1D electron gas model with umklapp scattering and pair breaking, as yielded by the renormalization group method detailed in the Appendix A. In Sec. IV, we discuss the results and their connection with theory. In Sec. V, we summarize and conclude this work.

II. EXPERIMENT

The present study is based on transport measurements of $(\text{TMTSF})_2(\text{ClO}_4)_{(1-x)}(\text{ReO}_4)_x$ single crystals grown electrochemically by Prof. K. Bechgaard in Copenhagen. All data have been taken at Orsay except for one $(\text{TMTSF})_2\text{ClO}_4$ sample already measured in a previous study at Kyoto⁴⁶ for its superconducting properties.

The measurement of the transverse resistivity ρ_{c^*} along the least conducting c^* direction has been privileged because of the requested quantitative comparison between samples with different ReO_4^- concentration. The frequent cracks occurring on cooling for the resistivity along a or b axes prevent any comparison between samples whereas ρ_{c^*} is known to be less influenced by such cracks even after multiple cooling processes⁴⁷. In addition, magnetoresistance measurements have shown that the band theory should apply below 10 K as also supported by the existence of a Drude edge along the c^* axis in the same temperature range⁴⁸. A previous comparative study of transport along a and c^* has shown that in spite of a very large anisotropy, electron scattering times measured along a or c^* exhibit a similar temperature dependence at least up to 30 K²³.

For $(\text{TMTSF})_2\text{ClO}_4$ samples studied in Kyoto, the resistivity was measured with the resistivity option of a PPMS with a dc current of $10\mu\text{A}$ reversed to cancel thermoelectric voltages [47]. For $(\text{TMTSF})_2(\text{ClO}_4)_{(1-x)}(\text{ReO}_4)_x$ studied in Orsay, a lock-in amplifier technique was used with an ac current of $10\mu\text{A}$ [30,31].

One of the major difficulties in interpreting low temperature transport in most $(\text{TMTSF})_2X$ superconductors is the existence of a negative curvature in the $R(T)$ curve approaching T_c below 4 K¹⁵. This negative curvature seems to be fairly robust as it can be observed even when SC is suppressed either by a magnetic field or in alloyed samples⁴⁹. While precursors due to SC could

contribute to a possible collective paraconductive contribution up to about $1.2 T_c$ ⁴⁹, there is still much uncertainty as to the origin of paraconductivity up to 3.5-4 K remaining a pending problem. Since precursor effects will not be discussed in the present article the analysis of the $\rho_{c^*}(T)$ curves has been limited to the range 4-10 K since our purpose is a study of the single particle non-Fermi liquid properties only.

The study of transport has been conducted in the alloys series $(\text{TMTSF})_2(\text{ClO}_4)_{(1-x)}(\text{ReO}_4)_x$ where the size of the ordered regions is controlled by the amount of the ReO_4^- substituent. The resistivity data are displayed on Fig. 1. We also emphasize that the samples on Fig. 1 have been labelled according to the nominal concentration of ReO_4^- which may differ significantly from the results obtained in an electron microprobe analysis⁵¹.

The resistivity of $(\text{TMTSF})_2\text{ClO}_4$ is *at variance* with that of $(\text{TMTSF})_2\text{PF}_6$ since no clear T -linear resistivity behavior is emerging from the raw data of $(\text{TMTSF})_2\text{ClO}_4$ ⁵⁰.

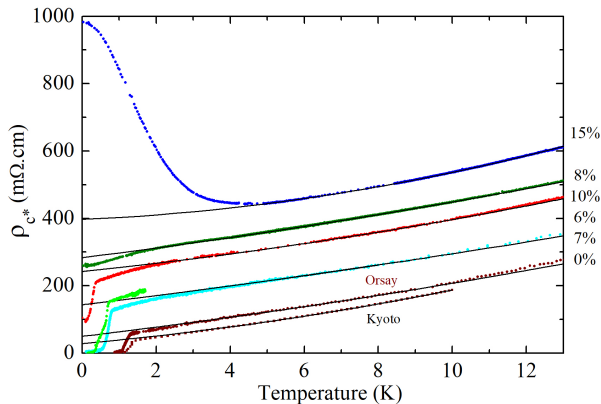


FIG. 1. Interlayer resistivity data for the $(\text{TMTSF})_2(\text{ClO}_4)_{(1-x)}(\text{ReO}_4)_x$ solid solutions all measured in the relax state and normalized to $28 \Omega\text{-cm}$ at ambient temperature. Samples have been labelled according to their nominal ReO_4^- concentration which may deviate in some cases from the actual defects concentration given by an electron microprobe analysis which in turn agrees with the value of the residual resistivity. The pure sample measured at Kyoto displayed a slightly smaller residual resistivity ($30 \text{ m}\Omega\text{-cm}$) than the Orsay one, ($50 \text{ m}\Omega\text{-cm}$). This is in line with $T_c = 1.35 \text{ K}$ at Kyoto while T_c is only 1.18 K in the Orsay sample.

Note that every sample on Fig. 1 differs by the behavior of their resistivity at low temperature. Both 0% samples exhibit a complete superconducting transition although their T_c and their residual resistivity ρ_{c^*0} are slightly different. The SC transition is still complete in the 7% sample. We also notice a complete transition for the 6% sample (green curve in Fig. 1) but the broadening at low temperature is a signature of a proximity effect between superconducting puddles⁴⁶. A further depression of T_c is observed in the 10% sample, but there the finite

zero temperature value of the resistivity suggests the existence of superconducting islands far from each other precluding global SC coherence through proximity effect. The 8% indicates the absence of any transition at finite temperature. The value of its ρ_{c^*0} appears to be reliable, although a tiny break in the $\rho_{c^*}(T)$ data (not visible on Fig. 1) occurring around 5 K made the polynomial analysis of the temperature dependence less reliable. In the 15% sample a metal-insulator transition is observed at 2.5 K which can be related to a SDW state occurring in anion-disordered sample after fast cooling²⁸. Similarly, the sample with a nominal concentration of 17% (not shown on Fig. 1 displays the onset of a SDW at 3.9 K.

The residual resistivity ρ_{c^*0} can be extracted relatively easily at different ReO_4^- concentrations from the data on Fig. 1, as it is only weakly dependent on the determination of the other prefactors in the polynomial fit (*vide infra*), but the correct analysis of the inelastic temperature dependence is a very delicate operation even in pure samples as already discussed in several previous publications^{21,23}.

The present study utilizes a polynomial fitting procedure keeping A and B fixed within the fitting window for each samples on Fig. 1. As it is difficult to put error bars on such fits we have privileged the data coming from three different fitting ranges between 4.5 K and 10 K leading to values for ρ_{c^*0} , A and B from the temperature dependence on Fig. 1 which are displayed on Fig. 2. The fitting window has been adequately chosen in order to avoid the onset of the as yet uncharacterized paraconductive contribution at low temperature and the proximity of the anion ordering at high temperature⁵². Transition temperatures defined by the onset tempera-

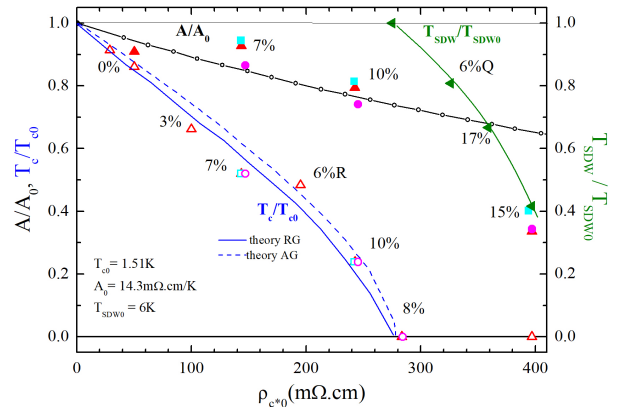


FIG. 2. T_c for the onset of superconductivity from experiment and theories and T_{SDW} versus the residual resistivity ρ_{c^*0} . Normalized value of A from the theory (open circles) and from the fits with different fitting ranges (red triangles 4.5-10 K, blue squares 5-9 K, magenta circles 5-10 K). A has been normalized to the value linearly extrapolated to $\rho_{c^*0} = 0$.

tures have been normalized to our highest observed transition for superconductivity namely, 1.51 K and to 6 K for the SDW transition as observed in case of strong anion

disorder⁵³. All samples on Fig. 2 refer to the very slowly cooled regime except for the 6% which has been measured both under relax and quenched conditions. The data of A for the 15% sample are departing from the slow decrease with x observed at lower concentrations. This may actually be the consequence of the resistivity upturn due to the SDW phase leading in turn to an underestimation of A using the present fitting window.

The x -axis of Fig. 2 refers to the residual resistivity as shown on the fits of Fig. 1 and not to the actual scattering rate. We do not expect this resistivity to be directly related to the elastic scattering rate whenever the conducting medium departs from homogeneity. This is likely true for the present data at high ReO_4^- concentrations when the superconducting transition becomes incomplete at say, 10%.

In the solid solution $(\text{TMTSF})_2(\text{ClO}_4)_{(1-x)}(\text{ReO}_4)_x$ two different anion order are competing according to x-ray diffuse scattering experiments^{41,42}. The (1/2, 1/2, 1/2) ReO_4^- ordering is responsible for a metal-insulator transition at 176 K in $(\text{TMTSF})_2\text{ReO}_4$ ³⁸ while the (0,1/2, 0) ClO_4^- ordering at 24 K folding the Q1D Fermi surface leads to a metallic phase at low temperature with a reduced value of the residual resistivity⁴⁶. At concentrations for x between 0 and 1, both anion orders are competing, but on the ClO_4^- rich side of the solid solution (0,1/2, 0) long-range order of ClO_4^- persists up to about $x = 3\%$ ^{41,42}. Increasing the ReO_4^- content further, the ClO_4^- ordering becomes short-ranged above 7% or so and a SDW ground state is stabilized instead of superconductivity²⁸. The picture which can be inferred from the x-ray analysis is thus an homogenous medium with local impurities at very low ReO_4^- concentration only becoming heterogenous above 3% where each impurity is surrounded by a disordered volume. The mean free path has been shown to be very large, of order of 1600 nm in a pristine sample^{46,54}. As the size of the ordered domains in alloys is likely to be much smaller than 1600 nm, we may assume that the mean free path in alloys is determined by the typical domain size. The predominant role of the domain size limiting the mean free path is also corroborated by a similar study performed on the solid solution $(\text{TMTSF})_2(\text{AsF}_6)_{(1-x)}(\text{SbF}_6)_x$ when the symmetry of the anions is central which has shown that even a 15% concentration of SbF_6 has no detectable effect on T_c ⁵⁵, being *at variance* with the present alloying effect in $(\text{TMTSF})_2\text{ClO}_4$.

The Abrikosov-Gorkov theory⁵⁶ of a conventional superconducting T_c in the presence of pair-breaking has also been reported on Fig. 2 together with the results of the renormalization group theory (Sec. III and Appendix A). We observe a satisfactory agreement between the onset temperatures and theories when the residual resistivity is considered as a representative of the scattering rate³². Such an agreement, however, may be surprising as the residual resistivity is the macroscopic resistivity of the entire sample which we found to become heterogenous at high ReO_4^- concentration, while T_c is the

onset transition temperature of well ordered domains. Consequently, this agreement between experiment and theories infers in turn the existence of some connection, $\rho_{c^*0} \propto 1/\lambda$, between the mean free path λ determined by domain size entering the theory and the macroscopic resistivity.

III. THEORY: RENORMALIZED LINEARIZED BOLTZMANN EQUATION FOR RESISTIVITY

In this section we sketch out the Boltzmann-RG approach to the calculation of electric resistivity in the presence of pair breaking. The calculation combines the linearized Boltzmann equation with the renormalization group method in the framework of the Q1D electron gas model for the Bechgaard salts²⁶. Prior to do so, it is important to draw attention on the fact that on experimental grounds, both longitudinal ($\Delta\rho_a$) and transverse ($\Delta\rho_{c^*}$) inelastic contribution to resistivity, though differing by a factor $\sim 10^4$ in amplitude for a compound like $(\text{TMTSF})_2\text{ClO}_4$, exhibit essentially the same temperature dependence below 30 K or so²³. Such a concurrence indicates that in this temperature range, they are apparently governed by the same scattering mechanism. In the following we shall then focus on the calculation of longitudinal resistivity for an array of weakly coupled chains in the ab plane perpendicular to the c direction.

We first consider the Boltzmann equation of the Fermi distribution function $f_{\mathbf{k}}$,

$$\left[\frac{\partial f_{\mathbf{k}}}{\partial t} \right]_{\text{coll}} = e\mathcal{E} \cdot \nabla_{\hbar\mathbf{k}} f_{\mathbf{k}}, \quad (1)$$

which stands for coherent carriers of charge e coupled to an external static electric field $\mathcal{E} = \mathcal{E}\hat{a}$. The collision term on the left depends on the interparticle (umklapp) scattering and collisions to impurities or defects. The linearization of the equation standardly proceeds by looking at small dimensionless deviations $\phi_{\mathbf{k}}$ to the equilibrium Fermi distribution function $f_{\mathbf{k}}^0 = 1/(e^{\beta\epsilon_{\mathbf{k}}} + 1)$, which in leading order yields the small variation $\delta f_{\mathbf{k}} \simeq f_{\mathbf{k}}^0(1 - f_{\mathbf{k}}^0)\phi_{\mathbf{k}}$. Here

$$\epsilon_{\mathbf{k}}^p = \hbar v_F(pk - k_F) - 2t_{\perp} \cos k_{\perp} d_{\perp} - 2t'_{\perp} \cos 2k_{\perp} d_{\perp} \quad (2)$$

is the electron spectrum of the Q1D electron gas model, where v_F is the Fermi velocity for right ($p = +$) and left ($p = -$) moving carriers along the chain, $\pm k_F$ are the 1D Fermi points in the absence of interchain hopping t_{\perp} ; the second nearest-neighbor interchain hopping term of amplitude t'_{\perp} acts as an antinegating term that simulates the effect of pressure in the model and d_{\perp} is the interchain distance along the b direction.

The linearization of (1) then yields

$$- \left[\frac{\partial \phi_{\mathbf{k}}}{\partial t} \right]_{\text{coll}} = \sum_{\mathbf{k}'} \mathcal{L}_{\mathbf{k}\mathbf{k}'} \phi_{\mathbf{k}'} = e\beta\mathcal{E} \cdot \mathbf{v}_{\mathbf{k}} \quad (3)$$

where $\mathbf{v}_{\mathbf{k}}$ is the carrier velocity in the $\hat{\mathbf{k}}$ direction. The collision operator is given by

$$\begin{aligned}
\mathcal{L}_{\mathbf{k}\mathbf{k}'} &= \mathcal{L}_{\mathbf{k}\mathbf{k}'}^u + \mathcal{L}_{\mathbf{k}\mathbf{k}'}^{\text{imp}} \\
&= \frac{(\pi\hbar v_F)^2}{(LN_P)^2} \sum_{\mathbf{k}_2, \mathbf{k}_3, \mathbf{k}_4} \frac{1}{2} |g_3(\mathbf{k}_F^p, \mathbf{k}_{F,2}^{p_2}; \mathbf{k}_{F,3}^{-p_3}, \mathbf{k}_{F,4}^{-p_4}) \\
&\quad - g_3(\mathbf{k}_F^p, \mathbf{k}_{F,2}^{p_2}; \mathbf{k}_{F,4}^{-p_4}, \mathbf{k}_{F,3}^{-p_3})|^2 \frac{2\pi}{\hbar} \delta_{\mathbf{k}+\mathbf{k}_2, \mathbf{k}_3+\mathbf{k}_4+p\mathbf{G}} \\
&\quad \delta(\varepsilon_{\mathbf{k}}^p + \varepsilon_{\mathbf{k}_2}^{p_2} - \varepsilon_{\mathbf{k}_3}^{p_3} - \varepsilon_{\mathbf{k}_4}^{p_4}) \\
&\quad \times \frac{f_{\mathbf{k}_2}^0 [1 - f_{\mathbf{k}_3}^0] [1 - f_{\mathbf{k}_4}^0]}{[1 - f_{\mathbf{k}}^0]} \\
&\quad \times (\delta_{\mathbf{k}, \mathbf{k}'} + \delta_{\mathbf{k}_2, \mathbf{k}'} - \delta_{\mathbf{k}_3, \mathbf{k}'} - \delta_{\mathbf{k}_4, \mathbf{k}'}) \\
&\quad + \frac{\pi\hbar v_F}{LN_P} \frac{2\pi}{\hbar} g_{\text{imp}}^2 \delta(\varepsilon_{\mathbf{k}}^p - \varepsilon_{\mathbf{k}'}^{p'}) (1 - \delta_{\mathbf{k}, \mathbf{k}'}), \tag{4}
\end{aligned}$$

where g_{imp}^2 is the square of the impurity scattering matrix element (normalized by $\pi\hbar v_F$) times the impurity concentration and N_P is the number of transverse momentum wave vectors. In the framework of the Q1D electron gas model, the electron-electron umklapp scattering amplitude is given by $g_3(\mathbf{k}_F^p, \mathbf{k}_{F,2}^{p_2}; \mathbf{k}_{F,3}^{-p_3}, \mathbf{k}_{F,4}^{-p_4})$ (normalized by $\pi\hbar v_F$). For an array of quarter-filled but weakly dimerized chains, this momentum dissipative process has its origin in the scattering of two carriers from one side of the Fermi surface to the other, which is made possible if momentum conservation in (4) involves the longitudinal reciprocal lattice vector $\mathbf{G} = (4k_F, 0)$ at half filling ($k_F = \pi/2a$). Umklapp scattering amplitude is evaluated on the Fermi surface sheets $\mathbf{k}_F^{\pm} = (k_F^p(k_{\perp}), k_{\perp})$, which is determined by the equation $\varepsilon_{\mathbf{k}_F}^p = 0$ and parametrized by the transverse wave vector k_{\perp} . As we will see below, its momentum dependent renormalization at temperature T , will be obtained by the RG technique at the one-loop level (see also Appendix A).

The longitudinal electric current is given by the expression in leading order

$$j_a \simeq \frac{2e}{LN_P d_{\perp}} \sum_{\mathbf{k}} v_F f_{\mathbf{k}}^0 (1 - f_{\mathbf{k}}^0) \phi_{k_{\perp}}, \tag{5}$$

where $\phi_{\mathbf{k}_F} \equiv \phi_{k_{\perp}}$ can be taken on the Fermi surface at low temperature. The conductivity σ_a or the inverse of the resistivity along the chains can then be written in the form

$$\sigma_a = \rho_a^{-1} = \frac{e^2}{c\hbar} \langle \bar{\phi}_{k_{\perp}} \rangle_{\text{FS}}, \tag{6}$$

where we have rescaled the deviation $\bar{\phi}_{k_{\perp}} = \phi_{k_{\perp}} / (\beta e \mathcal{E} d_{\perp})$ and inserted the lattice constant c in the c^* direction. Here $\langle \dots \rangle_{\text{FS}}$ corresponds to an average over the Fermi surface. Therefore the numerical solution of (3) for $\bar{\phi}_{k_{\perp}}$ using the momentum and temperature dependence of g_3 provided by the RG method leads to the resistivity as a function of the temperature²⁶.

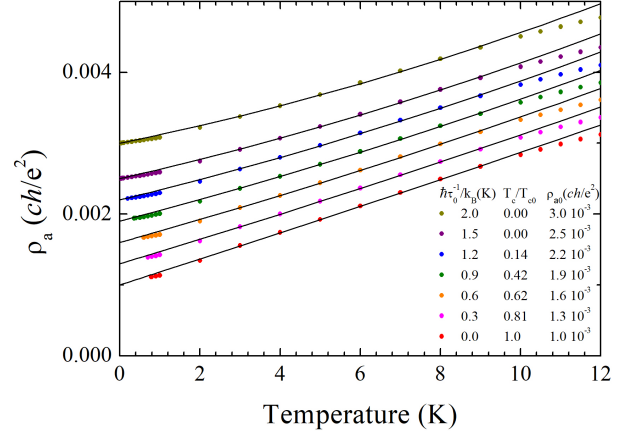


FIG. 3. Calculated temperature dependent resistivity as a function of pair-breaking parameter $\hbar\tau_0^{-1}/k_B$. The continuous lines are fits to the polynomial expression $\rho_a(T) = \rho_{a0} + AT + BT^2$.

We can complete the standard description of interactions in the Q1D electron gas model entering in the RG calculations of Appendix A. Thus besides the spectrum (2) and the aforementioned umklapp term, we have the backward and forward scattering amplitudes $g_1(\mathbf{k}_{F,1}^-, \mathbf{k}_{F,2}^+; \mathbf{k}_{F,3}^-, \mathbf{k}_{F,4}^+)$ and $g_2(\mathbf{k}_{F,1}^+, \mathbf{k}_{F,2}^-, \mathbf{k}_{F,3}^-, \mathbf{k}_{F,4}^+)$, also defined on the Fermi surface. For a superconducting compound like (TMTSF)₂ClO₄, which at ambient pressure is close to a magnetic QCP, typical values of the bare parameters of the model have been assessed in previous works^{19,26,57}. For example the Fermi temperature $T_F = \hbar v_F k_F / k_B \simeq 3000$ K and interchain hopping $t_{\perp} / k_B \simeq 200$ K are representative band parameters for the Bechgaard salts^{58,59}. The bare couplings (normalized by $\hbar\pi v_F$) we shall use are $g_1 = g_2/2 \simeq 0.32$ and $g_3 \simeq 0.033$, consistently with uniform susceptibility measurements and weak dimerization of the organic stacks. In these conditions the RG calculations for relatively weak antineesting parameter t'_{\perp} lead to SDW ordering temperatures that are compatible with those found in the antiferromagnetic Bechgaard salts at ambient pressure.

To suppress the SDW state and bring the system close to the QCP, t'_{\perp}/k_B is raised to 42 K or so, yielding a critical temperature $T_c^0 \sim 1$ K for (d-wave) superconductivity²⁶, which is congruent to the situation that prevails in (TMTSF)₂ClO₄ in slow cooling. This set of figures will fix the initial conditions with zero pair breaking effects ($\tau_0^{-1} = 0$) in the RG calculations [Eqs. (A1)] and the numerical solution of the Boltzmann equation (3). Finally a normalized impurity scattering matrix element $g_{\text{imp}}^2 = 0.001$ has been used in order to simulate a small residual resistivity term from (4); its value smoothly increases with τ_0^{-1} . It is worth noticing that the interplay between the impurity and inelastic parts in (4) has been found to be negligible.

In Figure 3 we show the resistivity calculated from Eqs. (6) and (A1) in the low temperature range down to the onset of critical superconducting domain occurring close to T_c where the renormalization flow goes to strong coupling.

Thus for zero pair breaking ($\tau_0^{-1} = 0$), the system is very close to the QCP and the resistivity becomes essentially T -linear up to 10 K or so where a crossover to a sublinear temperature dependence takes place (See⁶⁰). The origin T -linearity stems from the anomalous temperature dependence of umklapp scattering along the Fermi surface. Actually, despite the absence of SDW long-range order, spin correlations remain important and keep growing as temperature is lowered⁶¹. This derives from Cooper pairing terms in the RG flows (A1) which interfere constructively with the electron-hole (Peierls) pairing ones and then SDW fluctuations. This quantum fluctuation effect results in an anomalous temperature dependence of umklapp scattering that transforms the Fermi liquid quadratic T^2 dependence of resistivity into a T -linear behavior. Roughly speaking, the resistivity goes like $\rho_a \sim T^2 \langle g_3^2 \rangle_{\text{FS}}$ at low temperature where the mean-square value of umklapp scattering on the Fermi surface, which is representative of spin fluctuations, goes as $1/T$ at the critical t'_\perp .

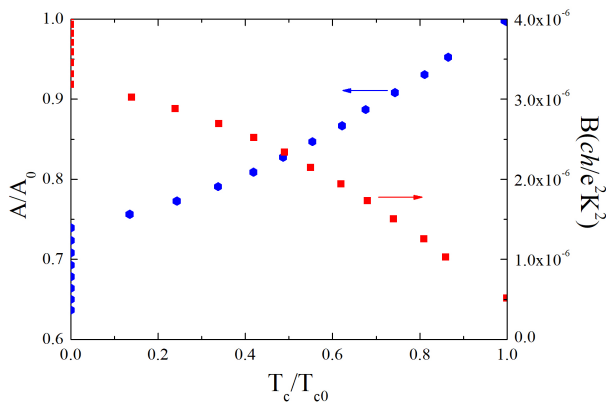


FIG. 4. A (left scale) and B (right scale) coefficients of the polynomial fit $\rho_a(T) = \rho_{a0} + AT + BT^2$ of the calculated resistivity (Fig. 3) as a function of T_c .

When pair-breaking τ_0^{-1} departs from zero, T_c gradually decreases and follows relatively closely the Abrikosov-Gorkov mean-field result down to the critical $\hbar\tau_0^{-1}/k_B \simeq 1.25$ K where $T_c \rightarrow 0$ (see Fig. 2). Concomitant with the fall of T_c , the temperature dependence of resistivity shows comparatively slow, albeit noticeable, alterations. We have proceeded to the fit of calculated resistivity curves of Fig. 3 to the polynomial form, $\rho_a = \rho_0 + AT + BT^2$, in the interval from 10 K down to the lowest temperature. According to Figure 4, the linear coefficient A of resistivity weakens with the size of τ_0^{-1} or the reduction of T_c . When $T_c \rightarrow 0$ as we approach the threshold τ_0^{*-1} , the reduction in the ratio

A/A_0 reaches about 25%; it continues a steady decrease beyond that point. As for the Fermi liquid BT^2 term of resistivity, it becomes visible and weakly grows, but regularly for $T_c/T_c^0 < 1$.

It follows that when pair breaking is present the scaling of A with T_c no longer holds. It must be stressed, however, that the threshold energy scale for pair-breaking $\hbar\tau_0^{*-1}$, which is of the order of $k_B T_c^0$, only affects electronic states within a narrow energy shell around the Fermi surface. Although the corresponding decline of the Cooper loop (\mathcal{L}_C) entering the RG flow (A1) is sufficient to suppress the instability against d -wave superconductivity, scattering processes taking place at higher energy distance from the Fermi surface remain virtually unaffected. These still contribute to the mixing of Cooper pairing and SDW correlations. The latter alongside umklapp scattering continue to be strong and are responsible for sustaining the amplitude of the T -linear coefficient of resistivity despite the absence of a finite T_c .

IV. DISCUSSION

Before we proceed with a comparison between theory and experiments in these alloys, it is important to notice that the present study is not dealing with a random distribution of strongly localized defects. Instead, we are facing a situation where the carrier life time in ordered regions is governed by the size of extended of disordered domains. The transport data showing the remittance of non superconducting domains at high ReO_4^- concentration suggest we are facing a problem of granular materials. Hence, the value of the residual resistivity cannot be simply extracted from the knowledge of the ReO_4^- concentration. The situation in the solid solution has similarities with that encountered in pure $(\text{TMTSF})_2\text{ClO}_4$ when the disorder is caused by rapid cooling of the sample⁴⁶. Therefore, we shall use a similar procedure to extract the fraction of the respective ordered and disordered regions from the resistivity data according to the effective-medium theory for a two-component conductor^{62,63},

$$1/\rho_{\text{eff}} = \left(p(1/\rho_{\text{Min}})^{1/3} + (1-p)(1/\rho_{\text{Max}})^{1/3} \right)^3, \quad (7)$$

where p is the volume fraction of the anion ordered domains. We take $\rho_{\text{Min}} = 50$ m Ω -cm according to the data on Fig. 1 and ρ_{Max} is given by $\rho_{\text{Max}} = \rho_{\text{Min}} + \Delta\rho_{c^*} = 280$ m Ω -cm where $\Delta\rho_{c^*}$ is the drop in residual resistivity coming from the anion ordering at 24 K which is known from the pure $(\text{TMTSF})_2\text{ClO}_4$ data ($\Delta\rho_{c^*} = 230$ m Ω -cm)⁴⁶. The derived values for p are displayed on Fig. 5. Using the value for the residual resistivity of sample 0% in Eq. (7) would provide $p=1$ for that sample in which the residual defects are not under control. As x-ray data have shown that full anion ordering does not exist even in pure and the best relaxed samples^{64,65}, we feel entitled to proceed differently for the determination of p in sample 0%. The derivation of p from Eq. (7) is expected

to become meaningful only in samples where the additional disorder provided by alloying is large compared to the residual disorder in a pristine sample. Therefore we have proceeded for p of the 0% sample with a linear interpolation between $\rho_{c^*0} = 0$ and $100 \text{ m}\Omega\cdot\text{cm}$ ($x = 3\%$) on Fig. 5 leading to the determination of p ($\simeq 0.78$) in the sample 0% of residual resistivity $\rho_{c^*0} = 50 \text{ m}\Omega\cdot\text{cm}$.

From Fig. 1, the 10% sample exhibits a superconducting transition ending at a finite value for the resistivity at zero temperature, which means that ordered regions are not percolant. Furthermore, in the 6% corresponding to $p = 0.18$ according to Fig. 5, the transition becomes complete meaning that pairing coherence becomes infinite. The volume fraction for ordered domains in 6% is smaller than the actual value expected for the percolation threshold, namely, $p = 0.3$ at which the first cluster of 3D ordered anions with infinite length develops⁶⁶. Such a situation can be understood taking into consideration the proximity effect which enables superconducting coherence over the entire volume even though ordered regions are still separated by small gaps of anion-disordered matter.

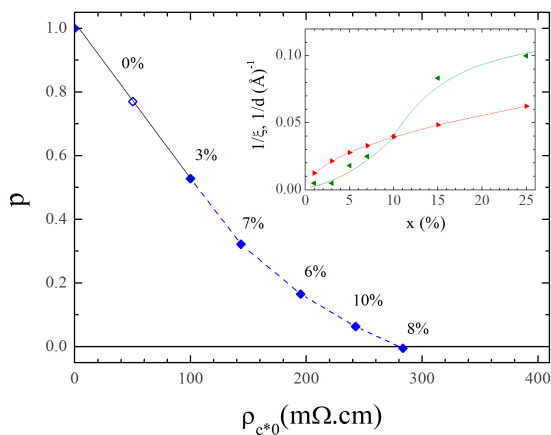


FIG. 5. The anion-ordered volume fraction p derived from the residual resistivity and the effective medium model. The insert shows the x dependence of the inverse correlation length for the $(0, 1/2, 0)$ ordering^{41,42} and the inverse length between ReO_4^- sites located at random. We note that around $x = 10\%$ the $(0, 1/2, 0)$ anion-ordered coherence length becomes shorter than the average distance between centers. It is above such a concentration that a granular behavior prevails. The superconducting coherence spreads over the whole volume in the 6% sample with $p = 0.18$ whereas the percolation threshold for ordered regions should arise around $p = 0.3$, *i.e.*, close to the 7% sample. This is a consequence of the proximity effect for superconductivity.

Regarding the SDW transition on Fig. 2, we note that the highest transition temperature at 6 K arises in a clean but already fully anion disordered sample⁵³. Hence, in a quenched state additional scattering coming from ReO_4^- anions is expected. This is the situation encountered in the quenched-6% samples where no $(0, 1/2, 0)$ order prevails because of the quenched state and additional scat-

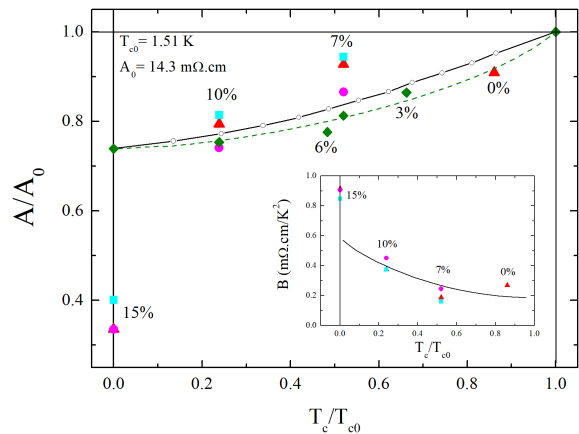


FIG. 6. Dependence of A/A_0 on T_c , from experiment and theory (full line). The colored square, triangle and circle symbols correspond to experimental data according to the different fitting ranges described in Fig. 2. The green diamonds are estimated A/A_0 derived from the two-conductor model Eq. (7) for the inelastic contribution. $A/A_0 = 0.75$ at $T_c = 0 \text{ K}$ and the volume fractions p according to Fig. 5 have been used. The green dotted line is a guide for the eye. Inset, displays the B dependence on T_c , the line is a guide for the eye.

tering coming from ReO_4^- substitution. As emphasized in Sec. III, non magnetic defects provide alongside antineesting some additional pair-breaking reducing density-wave correlations and then T_{SDW} – in the same way as non magnetic defects act in d -wave superconductors^{67–69}.

We can now plot the dependence of A on T_c , as shown on Fig. 6 comparing experimental data provided by the analysis of the resistivity of the metallic phase above T_c to the Boltzmann-RG calculation. We must be cautious because A is related to an homogenous medium in the two extreme cases of high and low T_c only where the sample is anion-ordered or disordered respectively but in-between (say, 7%) we face a more complex situation where A is related to the mixture of two metallic phases whereas T_c is given by the onset of superconductivity in the ordered phase only.

Experiments and theory of Fig. 4 agree on the fact that the suppression of A is no more than 25% once superconductivity in alloys is fully suppressed. In these conditions a sustained strength of a T -linear component for resistivity indicates that in the presence of non-magnetic pair-breaking the system moves away only slowly from the magnetic QCP. The amplitude of SDW correlations and with it the enhancement of umklapp scattering persist to a great extent in the anomalous temperature dependence of resistivity. Also satisfactory is the comparison between theory and experiments for the growth of the Fermi liquid B coefficient of resistivity, as displayed in Fig. 4 and the inset of Fig. 6. The rise of B as T_c decreases is steady, but its amplitude remains small.

Similarly, in case of pure $(\text{TMTSF})_2\text{ClO}_4$, the evolution of the T -linear term A as a function of the cooling rate can be extracted from a polynomial fit of the raw

data of previous works in Ref.⁴⁶, which we reproduce in Fig. 7 for representative cooling rates. The fit is in the window between 4.5 and 10 K, namely outside the paraconductive downturn of resistivity whose amplitude increases with the cooling rate. The suppression of A is at most 25% when the volume fraction of anion-ordered regions is monitored by the cooling rate leading to a complete suppression of T_c , as displayed on Fig. 8.

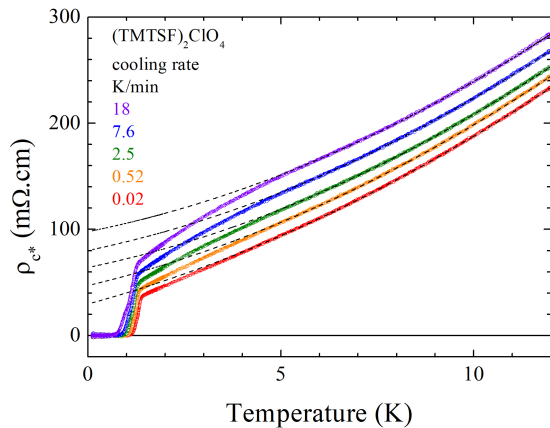


FIG. 7. $\rho_{c^*}(T)$ measured on $(\text{TMTSF})_2\text{ClO}_4$ and displayed in the temperature range between 12 K and the superconducting region for 0.020, 0.52, 2.5, 7.6, and 18 K/min cooling rates across the anion ordering transition. The same polynomial fitting procedure as for the data on Fig.1 has been used to extract the A , B and ρ_{c^*0} parameters at each cooling rates within the fitting window 5-10 K. The results are plotted as broken lines.

Finally, we comment on the behaviour of $\rho_{c^*}(T)$ in pristine $(\text{TMTSF})_2\text{ClO}_4$ at various cooling rates on Fig. 7. These data come from the extension to finite temperature of a previous work investigating residual resistivity and superconductivity in $(\text{TMTSF})_2\text{ClO}_4$ as the cooling rate is varied following a procedure already presented in Ref⁴⁶. The resistivity has been normalized to the value of $28 \Omega \cdot \text{cm}$ at ambient temperature following reports of previous $\rho_{c^*}(T)$ measurements^{30,46}. What is clear at first sight on Fig. 7 is the marked contrast between the strong effect of cooling rate on the residual resistivity and the much weaker effect on the inelastic part, a feature captured by the calculations of Sec. III.

The pure $(\text{TMTSF})_2\text{ClO}_4$ study⁴⁶ has shown that the material acquires a granular texture above a critical cooling rate of 1 K/mn where disordered regions separate anion-ordered domains in which bulk superconductivity arises and possibly spread over the whole sample via proximity effect. The volume fraction p related to ordered domains has been estimated at each cooling rates using the model of a two-component conductor⁴⁶. The data for the fitted values of A are displayed on Fig. 8 *versus* the anion-disordered volume fraction $1 - p$. A has been normalized to its value at the smallest cooling rate. We also show on the same Figure, the prediction of the effective medium model using Mathiessen's law applied

to the inelastic contribution, taking $A/A_0 = 1$ and 0.75 at $1 - p = 0$ and 1, respectively, following the results from the alloys series. The full squares with the dotted line are theoretical Boltzmann-RG points corrected for the evolution of the mean free path within each puddles at concentration p . These values provide an improvement for the agreement with the experimental data. The variation of the T -linear resistivity of the metallic phase above T_c at various cooling rates appears to be controlled nearly equally by life time and phase mixture effects.

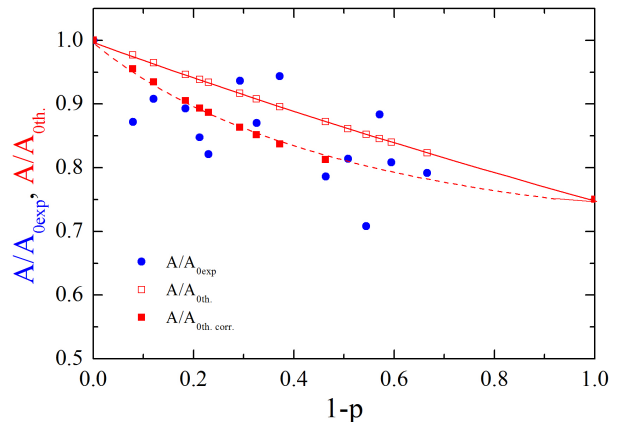


FIG. 8. Dependence of A/A_0 on the disordered volume fraction $1 - p$ in pure $(\text{TMTSF})_2\text{ClO}_4$ at various cooling rates, (blue dots). The model calculations for an effective conductor with $A/A_0 = 0.75$ at $p = 0$ are shown as red open squares. The model calculations taking into account the evolution of the mean free path in anion-ordered regions are the red full squares.

V. CONCLUSION

In this work, we have examined the influence of non-magnetic disorder generated by finite domains of anion ordering on the temperature dependence of resistivity in both $(\text{TMTSF})_2(\text{ClO}_4)_{1-x}(\text{ReO}_4)_x$ alloys and pristine $(\text{TMTSF})_2\text{ClO}_4$ at different cooling rates. These domains, presumably of different electronic structure, were found to have a strong impact on the onset of superconducting order. T_c is suppressed pointing to the existence of pair-breaking effects congruent with unconventional Cooper pairing. At variance with T_c , the pronounced T -linear resistivity in $(\text{TMTSF})_2\text{ClO}_4$ observed in slow cooling conditions does not reveal as a strong decline in alloying. A polynomial decomposition of resistivity temperature dependence has revealed that the linear term is not strongly weakened with x , indicating that quantum critical features remain strong despite the suppression of superconducting long-range order. The scaling between the T -linear term strength and T_c , which is seen under pressure in pure samples, was found to no longer hold as a function of disorder tuned by x or to a certain extent the cooling rate.

These results have been compared to a theoretical calculation based on the combination of the linearized Boltzmann equation of transport and the renormalization group approach to the umklapp vertex function. In the framework of the q1D electron gas model, we have shown that a range of relatively small energy scales for pair breaking is sufficient to instill a characteristic fall in the metallic instability against d-wave superconductivity. The calculated drop in T_c agrees with the one observed with x . Although small pair breaking energy is enough to suppress a scale like T_c , its impact on the strength of SDW fluctuations that feeds the amplitude of interparticle umklapp scattering remains relatively weak. The anomalous growth of umklapp at low temperature was found to be weakly altered along with linear resistivity term whose amplitude remains sizable, in agreement with experiment. Although the correlation between T_c and linear resistivity apparently breaks down, the correlation of the latter with spin fluctuations, which are the core of d -wave pairing, prevails.

ACKNOWLEDGMENTS

The samples studied for this work had been synthesized and grown by the late Professor Klaus Bechgaard. This work in France has been supported by CNRS and in Japan by Japan Society for the Promotion of Science (JSPS) Grant-in-Aids KAKENHI Grants No. JP26287078 and No. JP17H04848. C. B. thanks the National Science and Engineering Research Council of Canada (NSERC) and the Réseau Québécois des Matériaux de Pointe (RQMP) for financial support.

Computational resources were provided by the Réseau québécois de calcul de haute performance (RQCHP) and Compute Canada. A. Sedeki thanks the Institut Quantique (IQ) of the Université de Sherbrooke for its financial support.

Appendix A: Renormalization group equations for the electron gas with pair breaking effect

In this Appendix we give the one-loop RG flow equations for the momentum scattering amplitudes $g_{i=1,2,3}$ in the presence of pair breaking effects due to a finite lifetime τ_0 of the carriers. The RG approach to the quasi-1D electron gas is detailed in Refs^{19,61,70}. Each energy shell of thickness $\frac{1}{2}E_0(\ell)d\ell$, located at $\pm\frac{1}{2}E_0(\ell)$ from either sides of the Fermi sheets, is segmented into N_p patches, each centered at a particular value of the transverse momentum k_\perp , where $E_0(\ell) = E_0e^{-\ell}$ is the scaled bandwidth at step ℓ and $E_0 \equiv 2E_F$ is the initial bandwidth. The successive partial trace integration of electron degrees of freedom in the partition function leads to the renormalization or flow of the scattering amplitudes g_i as a function of ℓ . At the one-loop level, the flow combines corrections from the electron-hole (Peierls) and electron-electron (Cooper) interfering channels of scattering. Impurity (back) scattering introduces introduce pair breaking in the form of a carrier lifetime τ_0 in both $2\mathbf{k}_F$ electron-hole (Peierls)⁷¹ and (d-wave) Cooper⁷² channels. This leads to the flow equations for the $g_i(\mathbf{k}_{F1}^{p1}, \mathbf{k}_{F2}^{p2}; \mathbf{k}_{F3}^{p3}, \mathbf{k}_{F4}^{p4}) \rightarrow g_i(k_{\perp 1}, k_{\perp 2}, k_{\perp 3}, k_{\perp 4})$ on the Fermi surface, which can be written in the compact form

$$\begin{aligned} \partial_\ell g_1(k_{\perp 1}, k_{\perp 2}, k_{\perp 3}, k_{\perp 4}) &= (-2g_1 \circ g_1 + g_1 \circ g_2 + g_2 \circ g_1) \partial_\ell \mathcal{L}_P - (g_1 \circ g_2 + g_2 \circ g_1) \partial_\ell \mathcal{L}_C, \\ \partial_\ell g_2(k_{\perp 1}, k_{\perp 2}, k_{\perp 3}, k_{\perp 4}) &= -(g_1 \circ g_1 + g_2 \circ g_2) \partial_\ell \mathcal{L}_C + (g_2 \circ g_2 + g_3 \circ g_3) \partial_\ell \mathcal{L}_P, \\ \partial_\ell g_3(k_{\perp 1}, k_{\perp 2}, k_{\perp 3}, k_{\perp 4}) &= (-g_1 \circ g_3 - g_3 \circ g_1 + g_2 \circ g_3 + g_3 \circ g_2) \partial_\ell \mathcal{L}_P + 2g_2 \bullet g_3 \partial_\ell \mathcal{L}_P, \end{aligned} \quad (\text{A1})$$

where $\partial_\ell = \partial/\partial\ell$. $\mathcal{L}_{\nu=P,C}$ are the Peierls and Cooper loops whose derivative at finite temperature comprises an integration over the patch. These take the form

$$\begin{aligned} \partial_\ell \mathcal{L}_\nu(k_\perp, q_{\perp\nu}^{(\nu)}) &= \frac{E_0(\ell)}{4} \text{Re} \left\{ \sum_{\mu=\pm 1} \int_{k_\perp - \frac{\pi}{N_p}}^{k_\perp + \frac{\pi}{N_p}} \frac{dk_\perp}{2\pi} \right. \\ &\times \frac{\theta(|E_0(\ell)/2 + \mu A_\nu| - E_0(\ell)/2)}{E_0(\ell) + \mu A_\nu + i\hbar\tau_0^{-1}} \\ &\times \left[\tanh[\beta E_0(\ell)/4] + \tanh[\beta(E_0(\ell)/4 + \mu A_\nu/2)] \right] \left. \right\}, \end{aligned} \quad (\text{A2})$$

where

$$\begin{aligned} A_\nu(k_\perp, q_{\perp\nu}^{(\nu)}) &= -\epsilon_\perp(k_\perp) - \eta_\nu \epsilon_\perp(\eta_\nu k_\perp + q_{\perp\nu}^{(\nu)}) \\ &\quad + \eta_\nu \epsilon_\perp(\eta_\nu k_{\perp 2(4)} + q_{\perp\nu}^{(\nu)}) + \epsilon_\perp(k_{\perp 2(4)}) \end{aligned} \quad (\text{A3})$$

with

$$\epsilon_\perp(k_\perp) = -2t_\perp \cos k_\perp d_\perp - 2t'_\perp \cos 2k_\perp d_\perp$$

and $q_{\perp P}^{(\nu)} = k_{\perp 3} - k_{\perp 2} = k_{\perp 1} - k_{\perp 4}$ ($k_{\perp 3} - k_{\perp 1} = k_{\perp 2} - k_{\perp 4}$), $q_{\perp C} = k_{\perp 1} + k_{\perp 2} = k_{\perp 3} + k_{\perp 4}$; $\eta_P = 1$ and $\eta_C = -1$. $\theta(x)$ is the Heaviside function [$\theta(0) \equiv \frac{1}{2}$].

The momentum dependence of couplings in the discrete convolution products ‘ \circ ’ over the internal k_\perp loop variable on the right-hand side of (A1) are

in order $g(k_{\perp}, k_{\perp 4}, k_{\perp 1}, k_{\perp} - q_{\perp P})g(k_{\perp}, k_{\perp 2}, k_{\perp 3}, k_{\perp} - q_{\perp P})$ for the Peierls channel, $g(k_{\perp 1}, k_{\perp 2}, k_{\perp}, q_{\perp C} - k_{\perp})g(k_{\perp 3}, k_{\perp 4}, k_{\perp}, q_{\perp C} - k_{\perp})$ for the Cooper channel, and $g(k_{\perp}, k_{\perp 4}, k_{\perp 2}, k_{\perp} - q'_{\perp P})g(k_{\perp 1}, k_{\perp}, k_{\perp 3}, k_{\perp 1} - q'_{\perp P})$ for the \bullet product of the off-diagonal Peierls channel.

The integration of Eqs. (A1) up to $\ell \rightarrow \infty$ gives the values of the moment dependent scattering amplitudes g_i at temperature T . A singularity in the scattering amplitudes signals an instability of the electron gas against the formation of an ordering state at a critical temperature. For the band parameters and repulsive interactions fixed in Sec. III, the most probable instabilities are against either SDW or d-wave SC orderings. At low antinesting t'_{\perp} and zero pair breaking $\tau_0^{-1} = 0$, an SDW instability occurs with a singularity in both g_2 and g_3 amplitudes at the modulation wave vector $\mathbf{q}_0 = (2k_F, q_{\perp P} = \pi)$ and $T_{\text{SDW}} \sim 10 - 20\text{K}$. By tuning the antinesting at the QCP

near $t'_{\perp}^* \simeq 42\text{K}$, the SDW is suppressed and the instability occurs in the d-wave superconducting channel at $T_c^0 \sim 1\text{K}$, which is associated to a singularity for both g_2 and g_1 couplings at zero Cooper pair momentum $\mathbf{q}_0 = (0, q_{\perp C} = 0)$, but with a cosine modulation in k_{\perp} space. T_c^0 stands as the maximum T_c^0 at $\tau_0^{-1} = 0$ which we liken to the situation of the pure and slowly cooled (TMTSF)₂ClO₄ compound.

By increasing τ_0^{-1} it is the weakening of the Cooper loop (\mathcal{L}_C) singularity in (A2) that affects the instability against d-wave superconductivity. T_c/T_c^0 goes down and follows relatively closely the mean-field Abrikosov-Gorkov result⁷² as shown in Fig. 2. The concomitant impact of τ_0^{-1} on the momentum and temperature profile of Umklapp scattering and in turn on resistivity as obtained from the Boltzmann equation (4) is discussed in Sections III and IV.

-
- ¹ M. R. Norman. The challenge of unconventional superconductivity. *Science*, 332:196, 2011.
- ² J. Paglione and R. L. Greene. High-temperature superconductivity in iron-based materials. *Nature Physics*, 6:645, 2010.
- ³ D. C. Johnston. The puzzle of high-temperature superconductivity in layered iron pnictides and chalcogenides. *Advances in Physics*, 59:803, 2010.
- ⁴ L. Taillefer. Scattering and pairing in cuprate superconductors. *Ann. Review. Condens. Matter. Phys.*, 1:51, 2010.
- ⁵ Y. Dagan, M. M. Qazilbash, C. P. Hill, V. N. Kulkarni, and R. L. Greene. Evidence for a quantum phase transition in Pr_{2-x}Ce_xCuO_{4-δ} from transport measurements. *Phys. Rev. Lett.*, 43:167001, 2004.
- ⁶ D. Jaccard, K. Behnia, and J. Sierro. Pressure induced heavy fermion superconductivity of CeCu₂Ge₂. *Phys. Letters A*, 163:475, 1992.
- ⁷ N. D. Mathur, S. R. Julian F. M. Grosche, I. R. Walker, D. M. Freye, R. K. W. Haselwimmer, and G. G. Lonzarich. Magnetically mediated superconductivity in heavy fermion compounds. *Nature*, 394:39, 1998.
- ⁸ K. Kanoda. Recent progress in NMR studies on organic conductors. *Hyperfine interactions*, 104:235, 1997.
- ⁹ S. Lefebvre, P. Wzietek, S. Brown, C. Bourbonnais, D. Jerome, C. Méziere, M. Fourmigué, and P. Batail. Mott transition, antiferromagnetism, and unconventional superconductivity in layered organic superconductors. *Phys. Rev. Lett.*, 85:5420, 2000.
- ¹⁰ R. H. Mackenzie. Similarities between organic and cuprate superconductors. *Science*, 278:820, 1997.
- ¹¹ K. Jin, N. P. Butch, K. Kirshenbaum, J. Paglione, and R. L. Greene. Link between spin fluctuations and electron pairing in copper oxide superconductors. *Nature*, 476:73, 2011.
- ¹² K. Bechgaard, C. S. Jacobsen, K. Mortensen, H. J. Pedersen, and N. Thorup. The properties of five highly conducting salts. *Solid State Comm.*, 33:1119, 1980.
- ¹³ C. Bourbonnais and D. Jerome. Interacting electrons in quasi-one-dimensional organic superconductors. In A. Lebed, editor, *The physics of organic superconductors and conductors*, page 357. Springer, New York, 2008.
- arXiv:cond-mat/0904.0617.
- ¹⁴ F. Steglich, J. Aarts, C. D. Bredl, W. Lieke, D. Meschede, W. Franz, and H. Schafer. Superconductivity in the presence of strong Pauli paramagnetism: CeCu₂Si₂. *Phys. Rev. Lett.*, 43:1892, 1979.
- ¹⁵ D. Jerome, A. Mazaud, M. Ribault, and K. Bechgaard. Superconductivity in a synthetic organic conductor (TMTSF)₂PF₆. *J. Phys. Lett. (Paris)*, 41:L95, 1980. <https://hal.archives-ouvertes.fr/jpa-00231730v1>.
- ¹⁶ J. C. Scott, H. J. Pedersen, and K. Bechgaard. Magnetic properties of the organic conductor bis-tetramethyltetraselenafulvalene hexafluorophosphate, (TMTSF)₂PF₆ : A new phase transition. *Phys. Rev. Lett.*, 45:2125, 1980.
- ¹⁷ A. Andrieux, D. Jerome, and K. Bechgaard. Spin-density wave ground state in the one-dimensional conductor (TMTSF)₂PF₆ : microscopic evidence from 77Se and 1H NMR experiments. *J. Physique Lettres*, 42:L 87, 1981. Open archive on HAL <http://hal.archives-ouvertes.fr/>.
- ¹⁸ D. Jerome. The physics of organic superconductors. *Science*, 252:1509, 1991.
- ¹⁹ A. Sedeki, D. Bergeron, and C. Bourbonnais. Extended quantum criticality of low-dimensional superconductors near a spin-density-wave instability. *Phys. Rev. B*, 85:165129, 2012.
- ²⁰ H.J. Schulz, D. Jerome, M. Ribault, A. Mazaud, and K. Bechgaard. Possibility of superconducting precursor effects in the quasi-one-dimensional organic conductors: theory and experiments. *J. Physique*, 42:991, 1981. Open archive on HAL <http://hal.archives-ouvertes.fr/>.
- ²¹ N. Doiron-Leyraud, P. Auban-Senzier, S. René de Cotret, C. Bourbonnais, D. Jérôme, K. Bechgaard, and L. Taillefer. Correlation between linear resistivity and T_c in the Bechgaard salts and the pnictide superconductor Ba(Fe_{1-x}Co_x)₂As₂. *Phys. Rev. B*, 80:214531, 2009.
- ²² N. Doiron-Leyraud, P. Auban-Senzier, S. René de Cotret, C. Bourbonnais, D. Jérôme, K. Bechgaard, and L. Taillefer. Linear-T scattering and pairing from antiferromagnetic fluctuations in the (TMTSF)₂X organic superconductors. *Eur. Phys. J. B*, 78:23, 2010.
- ²³ P. Auban-Senzier, D. Jérôme, N. Doiron-Leyraud, S. René

- de Cotret, A Sedeki, C Bourbonnais, L Taillefer, P Alemany, E Canadell, and K Bechgaard. The metallic transport of $(\text{TMTSF})_2X$ organic conductors close to the superconducting phase. *J. Phys.: Condens. Matter*, 23:345702, 2011.
- ²⁴ P. Coleman and A. J. Schofield. Quantum criticality. *Nature*, 433:226, 2005.
- ²⁵ H. Meier, P. Auban-Senzier, C. Pépin, and D. Jérôme. Resistor model for the electrical transport in quasi-one-dimensional organic $(\text{TMTSF})_2\text{PF}_6$ superconductors under pressure. *Phys. Rev. B*, 87:125128, 2013.
- ²⁶ M. Shahbazi and C. Bourbonnais. Electrical transport near quantum criticality in low-dimensional organic superconductors. *Phys. Rev. B*, 92:195141, 2015.
- ²⁷ M. Y. Choi, P. M. Chaikin, S. Z. Huang, P. Haen, E. M. Engler, and R. L. Greene. Effect of radiation damage on the metal-insulator transition and low-temperature transport in the tetramethyltetraselenofulvalinium PF_6^- salt $(\text{TMTSF})_2\text{PF}_6$. *Phys. Rev. B*, 25:6208, 1982.
- ²⁸ S. Tomić, D. Jerome D. Mailly, M. Ribault, and K. Bechgaard. Influence of the disorder potential of the anions on the ground state of the organic alloy $(\text{TMTSF})_2(\text{ClO}_4)_{(1-x)}(\text{ReO}_4)_x$. *J. Phys. Colloq.*, 44:C3-1075, 1983.
- ²⁹ N. Joo, P. Auban-Senzier, C.R. Pasquier, P. Monod, D. Jérôme, and K. Bechgaard. Suppression of superconductivity by non-magnetic disorder in the organic superconductor $(\text{TMTSF})_2(\text{ClO}_4)_{(1-x)}(\text{ReO}_4)_x$. *Eur. Phys. J. B*, 40:43-48, 2004.
- ³⁰ N. Joo, P. Auban-Senzier, C. Pasquier, D. Jérôme, and K. Bechgaard. Impurity-controlled superconductivity/spin density wave interplay in the organic superconductor: $(\text{TMTSF})_2\text{ClO}_4$. *Europhys. Lett.*, 72:645, 2005.
- ³¹ J Shinagawa, Y Kurosaki, F Zhang, C Parker, S E Brown, D Jérôme, K Bechgaard, and J B Christensen. Superconducting state of the organic conductor $(\text{TMTSF})_2\text{ClO}_4$. *Phys. Rev. Lett.*, 98(14):147002, 2007.
- ³² Y. Suzumura and H. J. Schulz. Thermodynamic properties of impure anisotropic quasi-one-dimensional superconductors. *Phys. Rev. B*, 39:11398, 1989.
- ³³ A. P. Mackenzie, R. K. W. Haselwimmer, A. W. Tyler, G. G. Lonzarich, Y. Mori, S. Nishizaki, and Y. Maeno. Extremely strong dependence of superconductivity on disorder in Sr_2RuO_4 . *Phys. Rev. Lett.*, 80:161, 1998.
- ³⁴ Y. Maeno, H. Hashimoto, K. Yoshida, S. Nishizaki, T. Fujita, J. G. Bednorz, and F. Lichtenberg. Superconductivity in a layered perovskite without copper. *Nature*, 372(6506):532, 1994.
- ³⁵ J. P. Pouget and S. Ravy. Structural aspects of the Bechgaard salts and related compounds. *J. Phys. I*, 6:1501, 1996.
- ³⁶ D. Lepevelen, J. Gaultier, Y. Barrans, D. Chasseau, F. Castet, and L. Ducasse. Temperature and pressure dependencies of the crystal structure of the organic superconductor $(\text{TMTSF})_2\text{ClO}_4$. *Eur. Phys. J. B*, 19:363, 2001.
- ³⁷ T. Takahashi, D. Jerome, and K. Bechgaard. An NMR study of the organic superconductor: $(\text{TMTSF})_2\text{ClO}_4$. *J. Physique*, 45:945, 1984. <https://hal.archives-ouvertes.fr/jpa-00209828v1>.
- ³⁸ R. Moret, J. P. Pouget, R. Comes, and K. Bechgaard. X-ray scattering evidence for anion ordering and structural distortions on the low temperature phase of di(tetramethyltetraselenafulvalenium)perhenate $(\text{TMTSF})_2\text{ReO}_4$. *Phys. Rev. Lett.*, 49:1008, 1982.
- ³⁹ J. P. Pouget, G. Shirane, K. Bechgaard, and J. M. Fabre. X-ray evidence of a structural phase transition in di-tetramethyltetraselenafulvalenium perchlorate $(\text{TMTSF})_2\text{ClO}_4$, pristine and slightly ReO_4 substituted samples. *Phys. Rev. B*, 27:5203, 1983.
- ⁴⁰ According to structural studies, the anion ordering inside the methyl group cavity is also accompanied by a shift of the anion itself either towards methyl groups for $(\text{TMTSF})_2\text{ClO}_4$ ^{36,73} or towards Se atoms of a donor for $(\text{TMTSF})_2\text{ReO}_4$ ³⁸.
- ⁴¹ S. Ravy, R. Moret, J. P. Pouget, and R. Comes. Competition between structural instabilities in organic conductors and superconductors. *Physica B*, 143:542, 1986.
- ⁴² V. Ilakovac, S. Ravy, K. Boubekour, C. Lenoir, and P. Batail J. P. Pouget. Substitutional disorder and anion ordering transition in the $(\text{TMTSF})_2(\text{ClO}_4)_{(1-x)}(\text{ReO}_4)_x$ solid solution. *Phys. Rev. B*, 56:13878, 1997.
- ⁴³ T. Takahashi, D. Jerome, and K. Bechgaard. Observation of a magnetic state in the organic superconductor $(\text{TMTSF})_2\text{ClO}_4$: influence of the cooling rate. *J. Phys. Lett.*, 43:L565, 1982. <https://hal.archives-ouvertes.fr/jpa-00232093/document/>.
- ⁴⁴ P. Garoche, R. Brusetti, and K. Bechgaard. Influence of the cooling rate on the superconducting properties of the organic solid di-tetramethyltetraselenafulvalenium-perchlorate, $(\text{TMTSF})_2\text{ClO}_4$. *Phys. Rev. Lett.*, 49:1346, 1982.
- ⁴⁵ S. Tomić, D. Jerome, P. Monod, and K. Bechgaard. EPR and electrical conductivity of the organic superconductor di-tetramethyltetraselenafulvalenium-perchlorate, $(\text{TMTSF})_2\text{ClO}_4$ and a metastable magnetic state obtained by fast cooling. *J. Phys. Lett.*, 43:839, 1982. <https://hal.archives-ouvertes.fr/jpa-00232133v1>.
- ⁴⁶ S. Yonezawa, C. A. Marrache-Kikuchi, K. Bechgaard, and D. Jerome. Superconductivity in a quasi-one-dimensional metal with impurities. *Phys. Rev. B*, 97:014521, 2018.
- ⁴⁷ J. R. Cooper, L. Forró, B. Korin-Hamzić, K. Bechgaard, and A. Moradpour. Magnetoresistance of the organic conducting tetramethyltetraselenafulvalene salts $(\text{TMTSF})_2\text{ClO}_4$ and $(\text{TMTSF})_2\text{PF}_6$: Search for the coherent-diffusive transition or localization effects with increasing temperature. *Phys. Rev. B*, 33:6810, 1986.
- ⁴⁸ W. Henderson, V. Vescoli, P. Tran, L. Degiorgi, and G. Grüner. Anisotropic electrodynamic of low dimensional metals: Optical studies of $(\text{TMTSF})_2\text{ClO}_4$. *Eur. Phys. J. B*, 11:365, 1999.
- ⁴⁹ P. Auban-Senzier, C. R. Pasquier, D. Jerome, and K. Bechgaard. Fluctuating spin density wave conduction in $(\text{TMTSF})_2X$ organic superconductors. *Europhys. Lett.*, 94:17002, 2011.
- ⁵⁰ In contrast to $(\text{TMTSF})_2\text{PF}_6$ a hydrostatic pressure does not allow to cross the QCP region in $(\text{TMTSF})_2\text{ClO}_4$. The QCP in $(\text{TMTSF})_2\text{ClO}_4$ is expected to be located at a negative pressure. This situation has been reproduced applying a uniaxial elongation to $(\text{TMTSF})_2\text{ClO}_4$ along its b' -axis leading in turn to a decrease of the unnesting parameter t'_\perp with the suppression of superconductivity and the concomitant recovery of an insulating state below 6K⁷⁴.
- ⁵¹ A determination of the anion concentration by electron microprobe analysis in $(\text{TMTSF})_2X$ solid solutions have shown that the final anion concentration may deviate up to 30% from the initial concentration in the electrochemical

- cell, (K. Bechgaard, private communication).
- ⁵² In a previous study the paraconductive contribution has been attributed to a fluctuating SDW⁴⁹. This is one among other possibilities which requires confirmation.
- ⁵³ Ya. A. Gerasimenko, S. V. Sanduleanu, V. A. Prudkoglyad, A. V. Kornilov, J. Yamada, J. S. Qualls, and V. M. Pudalov. Coexistence of superconductivity and spin density wave in $(\text{TMTSF})_2\text{ClO}_4$: Spatial structure of the two-phase state. Phys. Rev. B, 89:054518, 2014.
- ⁵⁴ S. Yonezawa, S. Kusaba, Y. Maeno, P. Auban-Senzier, C. Pasquier, and D. Jérôme. Magnetic-field variations of the pair-breaking effects of superconductivity in $(\text{TMTSF})_2\text{ClO}_4$. J. Phys. Soc. Jpn., 77:054712, 2008.
- ⁵⁵ Ola Traetteberg. Thesis. University of Paris-Sud, unpublished, 1993.
- ⁵⁶ A. A. Abrikosov and L. D. Gorkov. Contribution to the theory of superconducting alloys with paramagnetic impurities. Sov. Phys. JETP, 12:1243, 1961.
- ⁵⁷ M. Shahbazi and C. Bourbonnais. Seebeck coefficient in correlated low dimensional organic metals. Phys. Rev. B, 94:195153, 2016.
- ⁵⁸ P. M. Grant. Electronic structure of the 2:1 charge transfer salts TMTCF. J. Phys. Colloq., 44:C3 847, 1983.
- ⁵⁹ L. Ducasse, A. Abderrabba, J. Hoarau, M. Pesquer, B. Gallois, and J. Gaultier. Temperature dependence of transfer integrals in the $(\text{TMTSF})_2X$ and $(\text{TMTTF})_2X$ families. J. Phys. C, 19:3805, 1986.
- ⁶⁰ The crossover to the sublinear temperature dependence contrasts with observation of Figs. 1 and 7 where the resistivity is rather found to evolve towards a T^2 behavior outside the quantum critical domain at high temperature.
- ⁶¹ C. Bourbonnais and A. Sedeki. Link between antiferromagnetism and superconductivity probed by nuclear spin relaxation in organic conductors. Phys. Rev. B, 80:085105, 2009.
- ⁶² L. D. Landau and E. M. Lifshitz. Electrodynamical of Continuous Media. Pergamon Press, Oxford, 1960.
- ⁶³ M Creyssels, C Laroche, E Falcon, and B Castaing. Pressure dependence of the electrical transport in granular materials. Eur. Phys. J. E, 40(5):56, 2017.
- ⁶⁴ J. P. Pouget. Structural aspects of the Bechgaard and Fabre salts: An update. Crystals, 2:466, 2012.
- ⁶⁵ An other sign supporting the existence of residual disorder in $(\text{TMTSF})_2\text{ClO}_4$ due to anions can be found in the NMR relaxation data in the superconducting state of $(\text{TMTSF})_2\text{ClO}_4$ recovering a Korringa-like relaxation namely the existence of a finite density of states at low temperature ascribed to residual disorder³¹.
- ⁶⁶ D. Stauffer and A. Aharony. Introduction to percolation theory. Taylor and Francis, London, 1994.
- ⁶⁷ S. Chang and K. Maki. Anion ordering and superconducting and spin-density wave transition temperatures in Bechgaard salts. Phys. Rev. B, 34:147, 1986.
- ⁶⁸ B. Dora, A. Virosztek, and K. Maki. Impurity effects in unconventional density waves in the unitary limit. Phys. Rev. B, 68:075104, 2003.
- ⁶⁹ The influence of the anion potential has been studied on the SDW state of $(\text{TMTSF})_2(\text{AsF}_6)_{(1-x)}(\text{SbF}_6)_x$ where the question of anion symmetry is irrelevant showing a 7% decrease of the transition temperature in a 50% solid solution⁵⁵.
- ⁷⁰ J. C. Nickel, R. Duprat, C. Bourbonnais, and N. Dupuis. Superconducting and density-wave instabilities in quasi-one-dimensional conductors. Phys. Rev. B, 73:165126, 2006.
- ⁷¹ B. R. Patton and L. J. Sham. Fluctuation conductivity in the incommensurate Peierls system. Phys. Rev. Lett., 33:638, 1974.
- ⁷² Y. Sun and K. Maki. Impurity effects in d -wave superconductors. Phys. Rev. B, 51:6059, 1995.
- ⁷³ P. Alemany, J. P. Pouget, and E. Canadell. Electronic structure and anion ordering in $(\text{TMTSF})_2\text{ClO}_4$ and $(\text{TMTSF})_2\text{NO}_3$: A first-principles study. Phys. Rev. B, 89:155124, 2014.
- ⁷⁴ H. Kowada, R. Kondo, and S. Kagoshima. Development of uniaxial elongation method and its application to low dimensional conductors. J. Phys. Soc. Jpn., 76:114710, 2007.